# Material and nanomechanical properties of bone structural units of cortical and trabecular iliac bone tissues from untreated postmenopausal osteoporotic women

Delphine Farlay, Guillaume Falgayrac, Camille Ponçon, Sébastien Rizzo, Bernard Cortet, Roland Chapurlat, Guillaume Penel, Isabelle Badoud, Patrick Ammann, Georges Boivin

Bone Reports 17 (2022) 101623

Contents lists available at ScienceDirect

Bone Reports

journal homepage: www.elsevier.com/locate/bonr

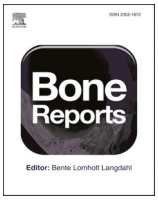

# Material and nanomechanical properties of bone structural units of cortical and trabecular iliac bone tissues from untreated postmenopausal osteoporotic women

Delphine Farlay [a,*], Guillaume Falgayrac [b], Camille Ponçon [a], Sébastien Rizzo [a], Bernard Cortet [b], Roland Chapurlat [a], Guillaume Penel [b], Isabelle Badoud [c], Patrick Ammann [c], Georges Boivin [a]

[a] INSERM, UMR 1033, Univ Lyon, Université Claude Bernard Lyon1, F-69008 Lyon, France
[b] Univ. Lille, CHU Lille, Univ. Littoral Côte d'Opale, ULR 4490 - MABLab- Adiposité, Médullaire et Os, F-59000 Lille, France
[c] Division of Bone Diseases, Department of Internal Medicine Specialties, Geneva University Hospital, 4rue Gabrielle-Perret-Gentil, CH-1211 Geneva 14, Switzerland

ARTICLE INFO

*Keywords:*
Bone intrinsic properties
Nanomechanical properties
Cortical/trabecular bone
Nanoindentation
Infrared spectroscopy
Raman spectroscopy

ABSTRACT

The differences in bone nanomechanical properties between cortical (Ct) and trabecular (Tb) bone remain uncertain, whereas knowing the respective contribution of each compartment is critical to understand the origin of bone strength. Our purpose was to compare bone mechanical and intrinsic properties of Ct and Tb compartments, at the bone structural unit (BSU) level, in iliac bone taken from a homogeneous untreated human population.

Among 60 PMMA-embedded transiliac bone biopsies from untreated postmenopausal osteoporotic women (64 ± 7 year-old), >2000 BSUs were analysed by nanoindentation in physiological wet conditions [indentation modulus (elasticity), hardness, dissipated energy], by Fourier transform infrared (FTIRM) and Raman microspectroscopy (mineral and organic characteristics), and by X-ray microradiography (degree of mineralization of bone, DMB). BSUs were categorized based on tissue age, osteonal (Ost) and interstitial (Int) tissues location and bone compartments (Ct and Tb).

Indentation modulus was higher in Ct than in Tb BSUs, both in Ost and Int. dissipated energy was higher in Ct than Tb, in Int BSUs. Hardness was not different between Ct and Tb BSUs. In Ost or Int BSUs, mineral maturity (conversion of non-apatitic into apatitic phosphates) was higher in Ct than in Tb, as well as for collagen maturity (Ost). Mineral content assessed as mineral/matrix (FTIRM and Raman) or as DMB, was lower in Ct than in Tb. Crystallinity (FTIRM) was similar in BSUs from Ct and Tb, and slightly lower in Ct than in Tb when measured by Raman, indicating that the crystal size/perfection was quite similar between Ct and Tb BSUs. The differences found between Ost and Int tissues were much higher than the difference found between Ct and Tb for all those bone material properties. Multiple regression analysis showed that Indentation modulus and dissipated energy were mainly explained by mineral maturity in Ct and by collagen maturity in Tb, and hardness by mineral content in both Ct and Tb.

In conclusion, in untreated human iliac bone, Ct and Tb BSUs exhibit different characteristics. Ct BSUs have higher indentation modulus, dissipated energy (Int), mineral and organic maturities than Tb BSUs, without difference in hardness. Although those differences are relatively small compared to those found between Ost and Int BSUs, they may influence bone strength at macroscale.

## 1. Introduction

Cortical bone (Ct) plays a central role in the bone strength, as it represents approximately 80 % of the bone mass. Trabecular bone (Tb) is also organized to distribute the forces and to optimize load transfer (rods and plates). Thus, both are required for the bone strength. Tb has a larger surface exposed to the bone marrow and is more metabolically active than Ct. Some medications act differently according to the type of envelope considered (Lespessailles et al., 2016). The macromechanical properties of Ct and Tb tissues are strongly influenced by the intermediate level of organization of bone, the bone structural units (BSUs). Ct and Tb bone are composed by a mix of BSUs, which can be distinguished

* Corresponding author.
*E-mail address:* delphine.farlay@inserm.fr (D. Farlay).

https://doi.org/10.1016/j.bonr.2022.101623
Received 22 July 2022; Received in revised form 23 September 2022; Accepted 26 September 2022
Available online 29 September 2022

into 2 main categories: osteonal BSUs (newly formed bone) and interstitial BSUs (older bone). The greater stiffness of Ct envelope than Tb envelope (Bayraktar et al., 2004) is generally associated to its structure and high mineralization, as it has a greater proportion of Interstitial (Int) BSUs than Tb. At the microscopic level, the structure of BSUs differs between Ct (osteons) and Tb (packets). In Ct, BSUs are formed by several concentric lamellae with different collagen fibrils orientations (Ascenzi and Bonucci, 1968), arranged around a central Haversian canal and oriented along the long bone axis. Osteons (recent bone) are separated by Int bone (old osteons) partially remodeled, bounded by cements lines. In contrast, Tb packets are composed of layers of parallel lamellae to Tb surfaces, oriented in different directions, and separated by Int bone. Thus, the structure of Tb makes it difficult to analyse and the different orientations of the trabeculae in space compound the comparison with Ct. The difference in mechanical properties at the BSUs scale between Ct and Tb are thus less documented, due to the complexity of hierarchical structure of bone, and to the difficulty of analysing similar structures between the 2 bone envelopes.

The intrinsic composition of BSUs, consisting in the deposition of organic matrix (collagen and non-collagenous proteins) covered by a mineral phase, is different between recent and old Int BSUs. Mineral is a major determinant of bone stiffness whereas collagen quality and orientation of collagen fibrils is rather associated to the toughness by providing the ductility and ability to absorb energy (Viguet-Carrin et al., 2006). The primary mineralization starts 5–10 days after the deposition of organic matrix (mainly type I collagen) by osteoblasts, and the mineral content reach 50–70 % of its maximal value (Boivin and Meunier, 2003; Boivin et al., 2008a; Roschger et al., 2008; Bala et al., 2013). Bone mineral is composed of a poorly crystallized calcium deficient apatite [mainly $Ca^{2+}$ (40 wt%), $PO_4^{3-}$ (18 wt%), $CO_3^{2-}$(6–7 wt%)], and other minor elements as citrate (1.5–2 wt%) and trace elements. The deposition of mineral phase, the crystal growth/size, and the stabilization of the apatite crystals are controlled by non-collagenous proteins [bone sialoprotein, osteopontin (OPN), osteocalcin (OC), glycosaminoglycans (GAG), proteoglycans (PG) …] (Fisher et al., 2001; Hunter and Goldberg, 1993), and also by ions (citrate ions) (Qiu et al., 2004; Hu et al., 2010; Davies et al., 2014). Then the speed of mineralization strongly decreases (secondary mineralization), and mineral crystals (apatite) begins a slow maturation, on the year-scale, with increase in crystals number, in maturation (conversion of non-apatitic precursors in the hydrated layer surrounding the crystal core containing apatitic domains), and in crystal size/perfection (crystallinity) (Bala et al., 2013; Farlay et al., 2010; Cazalbou et al., 2004). The secondary mineralization continues until the maximal degree of mineralization is reached. As the mineralization increases, the water content decreases, because the apatite crystals replaced some of the molecules of water as they growth. Several types of water coexist in bone matrix, freely mobile water (into vascular lacunar canalicular spaces), and bound water, with water bound to either the collagen network and/or to the mineral (Nyman et al., 2006a; Granke et al., 2015). In mineral, water is bound to the surface of bone crystals and located within the apatite lattice (structural water). The collagen bound water play an important role in mechanical properties of bone, as it confers to type I collagen its ductility and thus provides post-yield toughness to bone, and provides strength and toughness to mineral (Nyman et al., 2006a). In contrast, water bound to the mineral contributes to the orientation of apatite crystals during the process of mineralization (Wang et al., 2013). Moreover, enzymatic cross-linking, with intermolecular and interfibrillar cross-links which stabilize collagen fibrils, provides toughness to bone tissue. Compared to Int BSUS, recent BSUs are weakly mineralized (Boivin and Meunier, 2003; Boivin et al., 2008b), have a higher water content, higher non-collagenous proteins (NCPs) as OC and OPN levels (Sroga et al., 2011), and higher mature enzymatic cross links levels (Sroga et al., 2011; Nyman et al., 2006b).

The determination of micro- and nanomechanical properties has been largely studied in human Ct bone (Ascenzi and Bonucci, 1968; Lefèvre et al., 2019; Bala et al., 2011; Currey, 2002), but only few data are available for Tb (Boivin et al., 2008b; Zysset, 2009; Zysset et al., 1999; Turner et al., 1999; Rho et al., 1997; Hoffler et al., 2000). Currently, and maybe because they are influenced by several variables, such as type of bone (weight or non-weight bearing bones), orientation (Zysset et al., 1999; Wolfram et al., 2010) (transverse or longitudinal direction), chronological age (Mirzaali et al., 2016; Singleton et al., 2021), age of bone tissue (Ost vs Int) (Singleton et al., 2021), scale level (BSUs, lamellae (Zysset, 2009)), testing conditions (dry or wet (Wolfram et al., 2010)), no obvious distinction has been shown between the nanomechanical properties of Ct and Tb by nanoindentation. Several studies showed that elasticity was higher in Ct than Tb (Zysset et al., 1999; Rho et al., 1997; Rho et al., 1999a; Fan et al., 2006; Rho et al., 1999b; Fan et al., 2007), while others showed the inverse or no difference (Hengsberger et al., 2001; Roy et al., 1999). Elastic modulus correlates with the hardness (Zysset et al., 1999), is influenced by the mineral content, but not always. The difference in composition of bone matrix is thus crucial to understand the origin the nanomechanical properties. Dissipation of energy is also a mechanism protecting the bone from fracture, allowing to absorb energy produced during a stress. Creation of microcracks is one of the mechanisms allowing to dissipate energy (Burr, 2011). At the nanoscale level, deformation mechanisms such as sliding and mineral dissociation, interactions between mineral-collagen fibrils, mineral-mineral, collagen-NCPs, formation of sacrificial bonds, allow to create a large energy dissipation without compromising the integrity of the bone matrix (Fantner et al., 2005; Depalle et al., 2016).

The hypothesis of this study was that Ct bone, at equivalent bone tissue age, has higher mechanical, mineral and organic properties (mineralization, mineral and collagen maturity, crystallinity) than Tb bone. The aim was thus to compare the bone intrinsic and mechanical properties of Ct and Tb bone from untreated postmenopausal osteoporotic (PMOP) women at the BSU level, the intermediary level of organization of bone. We have analysed one type of bone (transiliac bone biopsies). It is important to emphasize that the aim was not to compare the global mechanical behaviour of Ct and Tb bone (themselves composed for different amounts of Ost and Int bone) but to compare the intrinsic and mechanical properties at the BSUs level.

## 2. Material and methods

### 2.1. Bone samples (Fig. 1)

Sixty transiliac bone biopsies from untreated postmenopausal osteoporotic women (mean ± SD: 64 ± 7 year-old) came from a phase III, multicenter, international, randomized double-blind, double-dummy (protocol CL3-12911-025) in which the aim was to assess the effects of 6 and 12 months of strontium ranelate or alendronate (Chavassieux et al., 2014). Only the baseline biopsies (M0) were used in this study. The results after 12 months of treatment (M12) have been recently published (Falgayrac et al., 2021). All patients gave written informed consent and the study had received ethical review board approval. Bone specimens were embedded in methylmethacrylate after fixation in 70 % ethanol and dehydration in 100 % ethanol. Before starting to cut the blocks, the orientation of Haversian canals have been identified under microscope, and bone biopsies were cut perpendicularly to the Haversian canals with a diamond saw (Well, Escil, Chassieu, France). The first section was kept for Raman spectroscopy analysis (Fig. 1). Their surface was polished using abrasive paper with decreasing grains (30, 12, 3 and 0.3 μm). Then 150 μm-thick sections were cut with a precision diamond wire saw for the measurement of degree of mineralization of bone. Sections were manually ground progressively to 100 ± 1 μm, polished with an alumina suspension (Escil), and cleaned with an ultrasonic device (Elma, Singer, Germany). Then sections for histomorphometry were done (Chavassieux et al., 2014) with a microtome Polycut E (Reichert-Jung, Leica, Germany). Then, 2 μm-thick sections were performed for FTIRM analysis.

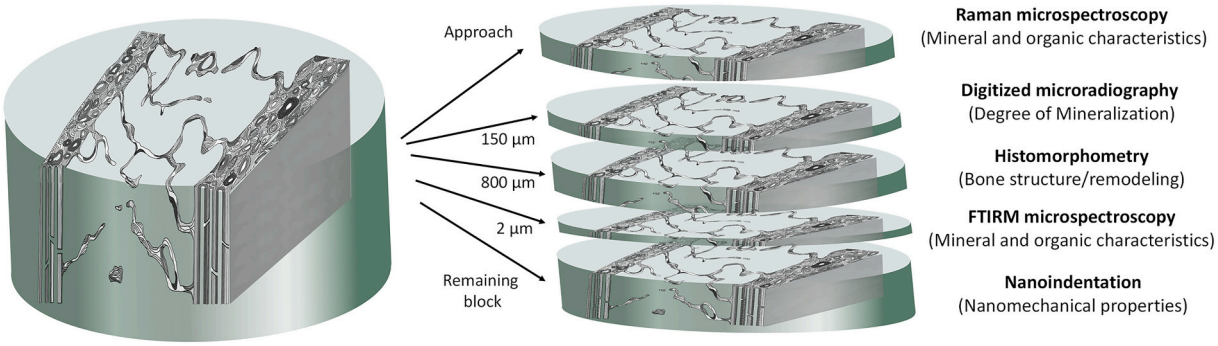


**Fig. 1.** Schematic bone biopsy illustrating the sequence of cutting for the different investigations of bone tissue.

Finally, the remaining block was used for nano-indentation analysis. Because nanoindentation is time consuming, only a part of the biopsies was analysed. These blocks were polished, finished with a 0.25 mm diamond solution, and were rehydrated in saline solution overnight at 4 degrees. Between the different matrices performed by the indenter, each specimen was kept immersed in physiological solution. Preliminary tests have shown that the values remained stable during measurements and checks are carried out during the process. Sixty bone biopsies were analysed by FTIRM and Raman, 50 by nanoindentation and 58 by digitized microradiography. As nanomechanical properties are strongly dependent from the orientation of bone (transverse or longitudinal direction), all the biopsies were cut transversally cut to Haversian canals, thus tested in longitudinal direction.

FTIRM and microradiographic analysis have been performed in our lab in Lyon (France), Raman spectroscopy in Lille (France), and nano-indentation in Geneva (Switzerland). For this reason, as the acquisitions had to be carried out simultaneously in different labs, we used different slides for each analysis. As it was not possible to perform all the analyses on the same BSUs, and as the objective was to categorize the "osteonal" and "interstitial" BSUs in Ct and Tb bone, we have chosen this order taking into account that the histomorphometry analysis had to be performed on the middle of the biopsy. In order not to lose material, we have chosen to use the 1st approach cut for Raman spectroscopy, the second for the X-ray microradiography (we needed a "parallel plane", always performed after a first approach cut). Histomorphometry was performed on the middle of the block. Finally, the FTIRM and the nanoindentation were done on adjacent block. So, the osteons tested by FTIRM and nanoindentation were on adjacent block in order to establish correlations.

### 2.2. Identification of bone of structural units (BSUs, Fig. 2)

The aim of the study was to compare the nanomechanical properties of Ost and Int BSUs, in both Ct and Tb bone, as well as their intrinsic properties at the BSU level. Due to organizational issues, it was not possible to target the same BSUs for the 4 techniques (nano-indentation, FTIRM, Raman, and microradiography). However, the following standardized protocol of identification of BSU was used for the 4 techniques. In Ct bone, osteonal BSUs (Ct Ost) were localized around Haversian canals (with a large diameter meaning the BSUs is forming) or on the endosteal area (Ct Int, Fig. 2). Old Int BSUs were localized between the osteonal BSUs, in the middle of the Ct bone. In Tb bone, recently formed bones packets (Tb Ost) were localized at the surface of the trabeculae. Old Int bone packets (Tb Int) were localized at the center of the trabeculae or in Tb nodes. The acquisitions in Ct and Tb bone by the different methodologies were distributed over the entire surface of each bone biopsy, to have an overall view of the biopsy.

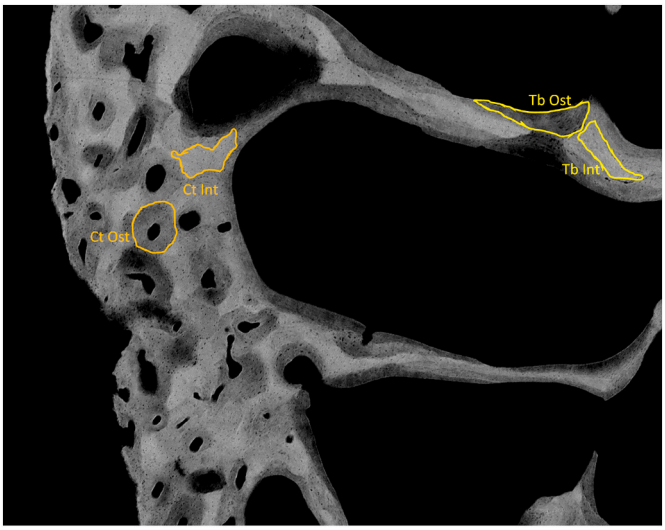


**Fig. 2.** Example of bone structural units (BSUs) selected for the degree of mineralization assessment, cortical osteonal (Ct Ost) and interstitial (Ct Int), BSUs in orange and trabecular osteonal (Tb Ost) and interstitial (Tb Int) BSUs in yellow. Analysis was performed in 4 categorized bone compartments: Ct Ost, Ct Int, Tb Ost, Tb Int.

### 2.3. Nanomechanical properties assessed by nano-indentation (Fig. 3)

Nano-indentation allows for assessment of the material level properties of bone tissue. Nano-hardness tester (NHT, CSM Instruments, Peseux, Switzerland) was used. The indenter tip is loaded at a given depth into the sample and the load is then held constant to creep the material below the tip. The protocol was described in previous works (Hengsberger et al., 2005; Ammann et al., 2007), and the curve force-displacement shown in Fig. 3. The indentation modulus is derived from the known properties of the indenter tip and the reduced modulus, and combines with the local elastic modulus and Poisson ratio of the specimen. Hardness is defined by an applied force P divided by contact area. The area of the hysteresis represented the energy dissipated to induce the plastic deformation.

Indentation modulus (GPa), hardness (MPa) and dissipated energy (pJ) of the bone were determined on rehydrated bone tissue samples. The mechanical tests were carried out on the categorized BSU, as previously described. Ten indents were performed in the Ct bone (5 in Ost and 5 in Int tissues) and 10 indents were also performed in Tb bone (Ost and Int tissues). As nano-indentation is time-consuming, 50 samples were analysed, and a total of 1000 BSUs were measured. The indents were set to a 900 nm depth with an approximate speed of 76 mN/min for both loading and unloading, and at maximum load, a 10 second holding period was applied. Finally, the limit of the maximal allowable thermal

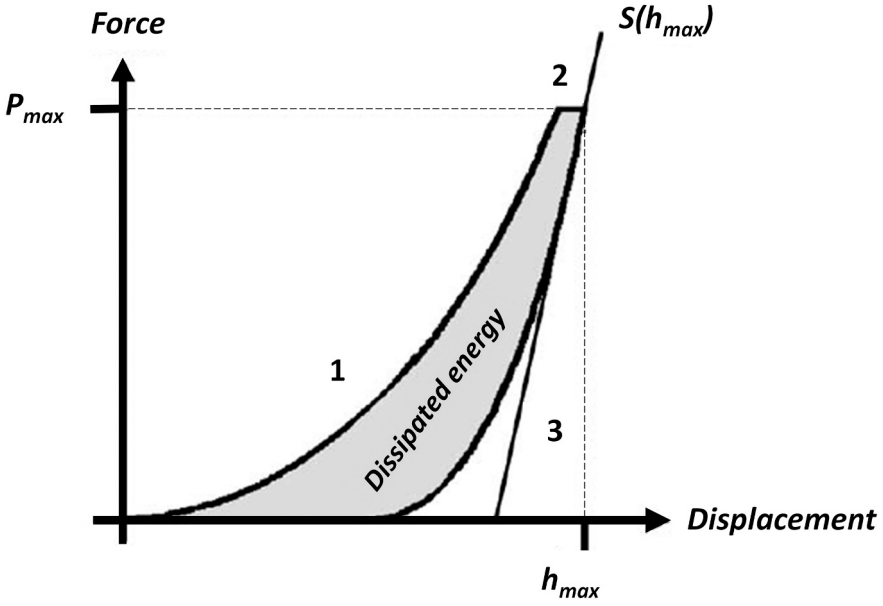


**Fig. 3.** Force-displacement curve of a nanoindentation test. (1) Loading, (2) holding, (3) unloading of the indenter tip. (Adapted from Ammann et al. (2007).)

drift was set to 0.1 nm/s.

### 2.4. Fourier transform infrared microspectroscopy (FTIRM, Fig. 4)

FTIRM analysis was performed on 2 μm-thick sections with a spectrometer Spectrum 100 coupled with an AutoImage GXII microscope (PerkinElmer GXII Auto-image Microscope) equipped with a wideband detector (mercury–cadmium–telluride) (7800–400 $cm^{-1}$). Each spectrum was collected at 45 × 35 μm spatial resolution with a 4 $cm^{-1}$ spectral resolution and an average of 50 scans, in transmission mode. Contributions of air and PMMA were subtracted from each spectrum and baseline was corrected. Ten spectra were performed in each Ct (5 in Ost and 5 in Int) and 20 in Tb bone (10 in Ost and 10 in Int), for a total of 40 measurements for each sample. As our microspectroscope is equipped with a wide range detector, no imaging data was available, as for classical imagers. Finally, each spectrum was deconvoluted by the "peak fitting" method using GRAMS/AI software (Thermo Galactic, Salem, NH, USA). Five variables were calculated: mineral/organic ratio (=mineral/matrix ratio, area under the curve $\nu_1\nu_3$ $PO_4$ (1184–910 $cm^{-1}$) over the amide I (1730–1592 $cm^{-1}$)); mineral maturity (ratio of the area under the curve $\nu_1\nu_3$ $PO_4$ at 1030 $cm^{-1}$ (apatitic phosphates) and area under the curve of $\nu_1\nu_3$ $PO_4$ at 1110 $cm^{-1}$ (non-apatitic phosphates)); crystallinity as the inverse of the width at half height of the peak at 604 $cm^{-1}$ ($\nu_4PO_4$); carbonation as the ratio of the area under the curve $\nu_2CO_3$ (862–894 $cm^{-1}$, types A + B + labile) over $\nu_1\nu_3PO_4$ (1184–910 $cm^{-1}$), and collagen maturity (area ratio 1660/1690 $cm^{-1}$) (Farlay et al., 2010; Farlay et al., 2011).

Sixty bone samples were analysed representing a total of 2400 BSUs analysed by FTIRM. Results were expressed as mean ± SD for each compartment: Ct Ost, Ct Int, Tb Ost, Tb Int.

### 2.5. Raman spectroscopy and physico-chemical variables (Fig. 4)

The Raman spectrometer was a LabRAM HR800 (HORIBA, Jobin-Yvon). The laser wavelength was 785 nm. The DuoScan mode was set to scan a surface of 30 × 30 μm in order to have a similar spatial resolution as in FTIRM analysis. Five spectra were acquired on surface bone from each Ct side and 10 in Tb surface bone, per sample. The same acquisition protocol was repeated on the Int bone for each biopsy which gives 20 measurements on Int bone (10 Ct and 10 Tb). A long acquisition time per spectrum of 30 s averaged over 4 acquisitions each was chosen, allowing to reduce fluorescence background and noise. A Savitzky−Golay smoothing filter (filter width: 3 and polynomial order: 2) was applied to the Raman spectra. The intensities and areas were integrated

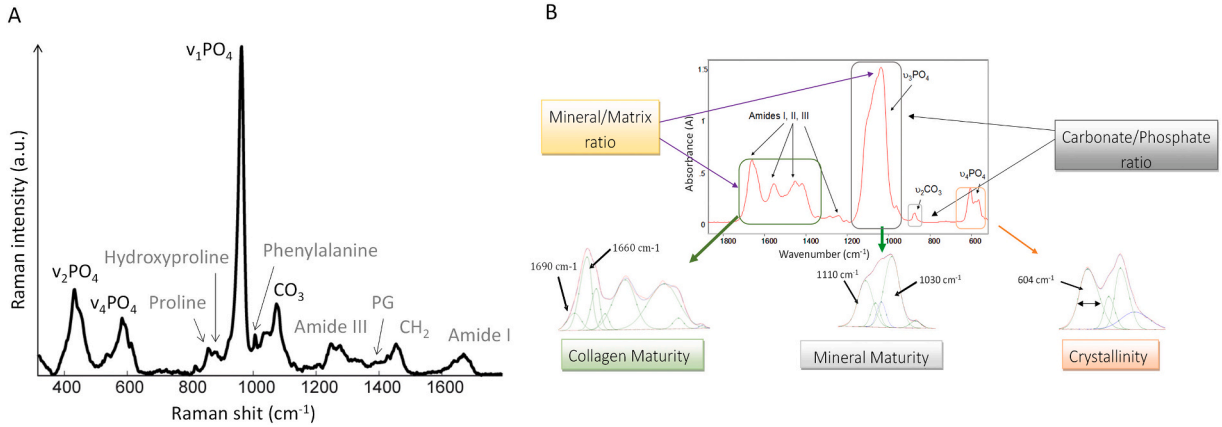


**Fig. 4.** Raman (A) and infrared (B) spectra obtained from human bone.

over local baseline using a sum filter. The filter calculates the intensities and areas within the chosen borders, and the background is subtracted by taking the baseline from the first to the second border (Falgayrac et al., 2012). The 6 physico-chemical variables (PPVs) were calculated per spectrum: the mineral/organic (=mineral/matrix) ratio as the intensity ratio of $\nu_1PO_4$ (960 $cm^{-1}$) over the $\delta(CH_2)$ (1450 $cm^{-1}$); the type-B carbonate substitution as the intensity ratio of B-type $CO_3^{2-}$ (1071 $cm^{-1}$) over $\nu_1PO_4$; crystallinity as the full width at half maximum intensity (FWHM) of the $\nu_1PO_4$; the hydroxyproline/proline ratio as the intensity ratio of hydroxyproline (871 $cm^{-1}$) over proline (854 $cm^{-1}$); the collagen maturity as the ratio between the intensity of 1670 $cm^{-1}$ over the area of amide I; the relative proteoglycan (PG) content as the ratio of areas of proteoglycan/$CH_3$ (1365–1390 $cm^{-1}$) over the amide III band (1243–1269 $cm^{-1}$) (Falgayrac et al., 2021). Sixty samples were analysed representing a total of 2400 BSUs analysed by Raman. Results were expressed as mean ± SD for each compartment: Ct Ost, Ct Int, Tb Ost, Tb Int.

### 2.6. Degree of mineralization of bone (DMB) assessed by digitized quantitative microradiography

The 100 ± 1 μm thick-sections were analysed by digitized X-ray microradiography (Montagner et al., 2015), with following exposure parameters: high voltage 40 kV, current 50 μA and power of 2 W. A Photonic science CCD camera FDI VHR 11 M with an active area of 36 × 24 mm (4008 × 2671 pixels) was used to detect the signal. The image digitization step was done with a 12-bit digital image detector (pixel size: 9 μm, object pixel size: 0.83 μm). An aluminium step-wedge reference composed of 8 steps (99.5 % pure foil; Strem Chemicals Inc., Bischheim, France) was exposed with the same exposure conditions, and gray level of each step were converted in g mineral/$cm^3$. Using the calibration curve constructed from the aluminium step-wedge, the gray levels measured on the bone X-ray images were converted in g mineral/$cm^3$, using code from MATLAB program (MathWorks, Natick, MA, USA). A threshold of 0.6 g/$cm^3$ was used. Individual BSUs (10 BSUs in each Ct with 5 in Ost and 5 in Int and 20 in Tb bone with 10 in Ost and 10 in Int) were selected on each sample, representing a total of 40 measurements for each sample. Results were expressed as mean ± SD for each compartment. In addition to this analysis by BSUs, we have also measured the whole Ct DMB and Tb DMB, as well as the heterogeneity index (HI = full-width at half-maximum of the curve of distribution) in order to compare the difference in DMB and the HI at the bone envelope level (tacking into account the proportion of Int and Ost BSUs).

### 2.7. Statistical analysis

Analyses were performed using SPSS® 16.0 (SPSS Inc., Chicago, IL), and a p-value $< 0.05$ was used to define statistical significance. Wilcoxon tests to compare the differences two by two, i.e., between Ct and Tb bone, Ost and Int tissues. Tb bone was taken as reference for the calculation of the percentage of difference between Ct and Tb. The mean percentage of difference between Ct and Tb was calculated as: (mean Ct − mean Tb) / mean Tb, in each bone compartment (Ost or Int).

A multiple regression analysis was used to quantify the contribution of mineral and organic variables (FTIRM) to the nanomechanical properties. The relationships between nanomechanical and intrinsic properties were tested using Pearson correlations. The normality of residuals was tested (Kolmogorov-Smirnov test). Residuals were gaussians excepted one for the hardness in Tb. However, an ordinal regression has been performed, which confirmed the results of the multiple linear regression.

## 3. Results

The aim of this study was to compare the nanomechanical properties of Ct and Tb BSUs, categorized by “tissue age”, in iliac bone biopsies from untreated postmenopausal osteoporotic women, and to explore their relationships with the matrix intrinsic properties. It is important to emphasize that this analysis was done at the BSU level, and not at the whole Ct and Tb bone scale (which are dependent of the amount of each BSUs). We used both FTIRM and Raman microspectroscopy due to their complementarity of information. Indeed, even if some variables are “equivalent”, as with the mineral/matrix ratio or crystallinity, some variables are given only by one methodology (mineral maturity, whole carbonates for example for FTIR, proline/hydroxyproline or PG/amide III by Raman spectroscopy).

### 3.1. Differences between cortical and trabecular BSUs (Table 1)

Differences were found between Ct and Tb BSUs. For each variable, the percentage of those differences was systematically compared to the difference found between Ost and Int BSUs.

Regarding the nanomechanical properties, the indentation modulus of Ct BSUs was higher than Tb BSUs in Ost (+17 %, $p < 0.0001$) and Int (+10.3 %; $p < 0.0001$). The dissipated energy of Ct BSUs was higher than Tb BSUs in Int (+3.6 %, $p < 0.0255$). For comparison, the difference in indentation modulus between Int and Ost was between +27.4 % ($p < 0.0001$) for Ct and + 35.6 % ($p < 0.0001$) for Tb bone. The difference in dissipated energy between Int and Ost was between +37 % ($p < 0.0001$) for Ct and + 36.4 % ($p < 0.0001$) for Tb bone.

No difference in hardness was found between Ct and Tb BSU, either in Ost or Int. The difference between Int and Ost was 46.5 % ($p < 0.0001$) and 55.1 % ($p < 0.0001$) in Ct and Tb for the hardness.

Regarding the mineral variables, Ct BSUs were less mineralized (X-ray microradiography) than Tb BSUs, both in Ost and Int (−2.9 %, $p < 0.0001$ and −0.9 %, $p < 0.027$). Same results were obtained by FTIRM and Raman spectroscopy on the mineral/matrix ratio (lower ratio in Ct than Tb BSUs (−2.1 % to −6.4 %, $p = 0.0092$ and $p < 0.0001$, respectively)), except for the Ost by FTIRM.

The differences in DMB between Ct and Tb BSUs were lower (2.9 % and 0.9 % of difference in Ost and Int, respectively) than those found between Ost and Int BSUs (15 % and 12 % of difference in Ct and Tb, respectively). In FTIRM and Raman spectroscopy, the difference in the mineral/matrix ratio between Ost and Int BSUs varied between 31.3 % and 53.3 %, with a level of significance of $p < 0.0001$ for all.

The DMB which was measured in the whole Ct and Tb envelopes (taking into account all the BSUs contribution in each envelope, thus the proportion of Ost and Int bone). The DMB was higher in whole Ct than in whole Tb bone (Table 1, 1.029 ± 0.043 g/$cm^3$, $p < 0.0001$ and 1.003 ± 0.031 g/$cm^3$, $p < 0.0001$ respectively). In contrast, the HI was the same between whole Ct and Tb bone (0.168 ± 0.025 g/$cm^3$, 0.168 ± 0.021 g/$cm^3$, NS, respectively).

Mineral maturity was significantly higher in Ct than Tb BSUs (FTIRM: + 10.3 % in Ost and +18.5 % in Int, $p < 0.0001$). For comparison, the difference between Int and Ost was 56.6 % ($p < 0.0001$) in Ct and 45.3 % ($p < 0.0001$) in Tb.

Crystallinity was the same between Ct and Tb BSUs measured by FTIRM and slightly different by Raman (−0.6 % in Ct Ost vs Tb Ost; +0.9 in Ct Int vs Tb Int). The difference between Ost and Int BSU varied between 4 and 7.7 % in Ct and Tb BSUs, with a level of significance of $p < 0.0001$ for all.

Total carbonation measured by FTIRM (Type A, B and labile carbonates) was lower in Ct than Tb BSUs, both in Ost and Int (−2.9 %, $p = 0.0007$ and −4.3 %, $p < 0.0001$, respectively). The difference between Ost and Int BSUs was 15.8 % and 14.7 %, $p < 0.0001$, in Ct and Tb respectively. Type-B carbonates measured by Raman was also lower in Ct than Tb BSUs, only in Int (−1.1 %, $p = 0.0003$). The difference between Ost and Int BSUs was +1.2 % ($p = 0.0053$) and +2.9 % ($p < 0.0001$), in Ct and Tb respectively.

Regarding the organic variables, collagen maturity (FTIRM) was higher in Ct than Tb BSU (+7.5 %, $p < 0.02$ in Ost, NS in Int). For comparison, the difference between Ost and Int BSUs varied between

**Table 1**
Variables reflecting bone quality and differences (expressed as %) between cortical and trabecular BSUs (bone structural units), in both osteonal and interstitial (white part). Differences between interstitial and osteonal BSUs, in cortical and trabecular (gray part). Bold numbers indicate a significant difference, and p-values are in italic.

| | Cortical Osteonal | Trabecular Osteonal | Difference (%) | p value | Cortical Interstitial | Trabecular Interstitial | Difference (%) | p value | Cortical interstitial vs osteonal | | Trabecular interstitial vs osteonal | |
|---|---|---|---|---|---|---|---|---|---|---|---|---|
| | | | | | | | | | % of difference | p value | % of difference | p value |
| **NanoIndentation (n = 50)** | | | | | | | | | | | | |
| Indentation modulus (GPa) | 10.50 (1.65) | 9.15 (1.52) | **+17%** | ***<0.0001*** | 13.26 (1.93) | 12.10 (1.42) | **+10.3%** | ***0.0001*** | **+27.4%** | ***<0.0001*** | **+35.6%** | ***<0.0001*** |
| Hardness (MPa) | 286 (34) | 278 (39) | +4% | *NS* | 414 (55) | 426 (66) | −1.6% | *NS* | **+46.5%** | ***<0.0001*** | **+55.1%** | ***<0.0001*** |
| Dissipated energy (pJ) | 2350 (357) | 2253 (258) | +5% | *NS* | 3147 (358) | 3041 (264) | +3.6% | ***0.0255*** | **+37%** | ***<0.0001*** | **+36.4%** | ***<0.0001*** |
| **FTIRM (n = 60)** | | | | | | | | | | | | |
| Mineral/matrix | 3.03 (0.38) | 3.10 (0.40) | −1.6% | *NS* | 4.49 (0.22) | 4.69 (0.30) | **−4.0%** | ***<0.0001*** | **+51.8%** | ***<0.0001*** | **+53.3%** | ***<0.0001*** |
| Mineral maturity | 1.47(0.26) | 1.35 (0.26) | **+10.3%** | ***<0.0001*** | 2.21 (0.24) | 1.87 (0.16) | **+18.5%** | ***<0.0001*** | **+56.6%** | ***<0.0001*** | **+45.3%** | ***<0.0001*** |
| Crystallinity (cm) | 0.0365 (0.0018) | 0.0365 (0.0018) | 0% | *NS* | 0.0392 (0.0012) | 0.0393 (0.0014) | 0% | *NS* | **+7.7%** | ***<0.0001*** | **+7.6%** | ***<0.0001*** |
| Total carbonates | 0.0080 (0.0010) | 0.0082 (0.0011) | **−2.9%** | ***0.0007*** | 0.0066 (0.0004) | 0.0070 (0.0004) | **−4.3%** | ***<0.0001*** | **−15.8%** | ***<0.0001*** | **−14.7%** | ***<0.0001*** |
| Collagen maturity | 2.70 (0.53) | 2.55 (0.51) | **7.5%** | ***0.0142*** | 4.25 (0.32) | 4.29 (0.29) | −1.2% | *NS* | **+62.8%** | ***<0.0001*** | **+75.4%** | ***<0.0001*** |
| **Raman (n = 60)** | | | | | | | | | | | | |
| Mineral/matrix | 5.90 (0.73) | 6.30 (0.65) | **−6.4%** | ***<0.0001*** | 8.04 (0.60) | 8.21 (0.60) | **−2.1%** | ***0.0092*** | **+38%** | ***<0.0001*** | **+31.3%** | ***<0.0001*** |
| Type-B carbonates | 0.1926 (0.0060) | 0.1919 (0.0061) | +0,5% | *NS* | 0.1950 (0.0065) | 0.1974 (0.0067) | **−1.1%** | ***0.0003*** | **+1.2%** | ***0.0053*** | **+2.9%** | ***<0.0001*** |
| Crystallinity (cm) | 0.0500 (0.0009) | 0.0503 (0.0008) | **−0.6%** | ***0.0002*** | 0.0528 (0.0008) | 0.0523 (0.0008) | **+0.9%** | ***<0.0001*** | **+5.65%** | ***<0.0001*** | **+4%** | ***<0.0001*** |
| Pro/hydroxypro | 1.4984 (0.0616) | 1.4892 (0.0527) | +0.6% | *NS* | 1.5221 (0.0760) | 1.5241 (0.0718) | −0.2% | *NS* | **−1.4%** | ***0.0432*** | **−2.1%** | ***0.0017*** |
| PG/amide III | 0.0921 (0.0157) | 0.0936 (0.014) | −1.6% | *NS* | 0.0830 (0.0140) | 0.0895 (0.0131) | **−5.9%** | ***<0.0001*** | **−8.6%** | ***<0.0001*** | **−10%** | ***0.0001*** |
| **X-ray microradiography (n = 58)** | | | | | | | | | | | | |
| DMB (g/cm$^3$) | 0.99 (0.05) | 1.02 (0.05) | **−2.9%** | ***<0.0001*** | 1.14 (0.04) | 1.15 (0.04) | **−0.9%** | ***0.027*** | **+15%** | ***<0.0001*** | **+12%** | ***<0.0001*** |
| | **Cortical** | **Trabecular** | | | | | | | | | | |
| Global DMB (g/cm$^3$) | 1.029 (0.043) | 1.003 (0.031) | **+2.6%** | ***<0.0001*** | | | | | | | | |
| Global HI (g/cm$^3$) | 0.168 (0.025) | 0.168 (0.021) | 0% | *NS* | | | | | | | | |

62.8 % and 75.4 % in Ct and Tb, respectively.

Pro/hydroxyproline measured by Raman was not different between Ct and Tb BSUs. A difference was found between Int and Ost of 1.4 % ($p = 0.0432$) and 2.1 % ($p = 0.0017$), respectively.

PG/amides III were lower in Ct than Tb BSUs, only in Int (−5.9 %, $p < 0.0001$), NS for Ost. For comparison, a difference of −8.6 % ($p < 0.0001$) and −10 % ($p < 0.0001$) was found between Int and Ost, in Ct and Tb, respectively.

### 3.2. Correlations between nanomechanical properties and intrinsic bone quality variables (Table 2 and Fig. 5)

Correlations were performed between the variables obtained by the different techniques separately in Ct (Ost + Int) and Tb (Ost + Int) (Table 2). The majority of variables were significantly correlated and mainly similar between Ct and Tb compartments. Indentation modulus, hardness and dissipated energy were positively correlated with mineral variables (IR-Raman mineral/matrix, IR-mineral maturity, IR-Raman crystallinity, DMB) and IR collagen maturity. They were negatively correlated with Raman pro/hydroxypro in Ct only, and with Raman PG/amides in both Ct and Tb. To better identify Ost and Int, Fig. 5 illustrates the correlations between nanoindentation (Indentation modulus, hardness and dissipated energy) with 3 FTIRM variables (mineral maturity, mineral/matrix and collagen maturity), with colored points separately in each of the 4 compartments.

### 3.3. Relationship between nanomechanical and intrinsic variables (Multiple Stepwise Regression Analysis) (Table 3)

The FTIRM and nanoindentation analysis were done on adjacent slices. Thus, BSUs analysed are from a similar region at the scale of the bone biopsy. For this reason, we explored the correlations between the nanoindentation and FTIRM variables, because the slices analysed by Raman were not adjacent with nanoindentation and FTIRM (~1 cm of thickness difference). In order to explain the contribution of bone material properties to nanomechanical variables, we used a multiple regression model, for Ct and Tb compartments. Four variables have been selected (among 5) to reflect the mineral content (mineral/matrix), maturation of mineral crystals sensitive to water (mineral maturity), one structural mineral parameter (crystallinity) and the organic variable (collagen maturity). Total carbonation was excluded from the model, as its significance is unclear as mentioned previously and to not disturb the model. Depending on the compartments, nanomechanical variables were explained by different intrinsic variables. Indentation modulus was explained first by mineral maturity then by crystallinity in Ct, and by first collagen maturity then mineral maturity in Tb. Hardness was explained first, both in Ct and Tb, by mineral/matrix ratio, and then by mineral maturity and crystallinity in Ct and Tb, respectively. Dissipated energy was explained by mineral maturity, collagen maturity and then crystallinity, whereas this was explained by first collagen maturity followed by mineral maturity in Tb.

## 4. Discussion

The aim of this study was to compare the intrinsic and nanomechanical properties of Ct and Tb bone of human iliac bone from 60 postmenopausal osteoporotic untreated women, at the BSU level. As it was not possible to apply the different methods on the same BSUs from an organizational point of view (4 techniques performed in 3 different laboratories), we categorized the BSUs in four groups, Ct Int, Ct Ost, Tb Int and Tb Ost. We found that Ct and Tb BSUs exhibit different characteristics. The hypothesis of the study was that Ct bone had higher mechanical, mineral and organic properties than Tb bone, at equivalent bone tissue age. Indeed, as 80 % of the bone mass is in the Ct bone, this later must be able to adapt and resist the various loads exerted on it. Although Tb bone also plays a role in bone strength by transferring surface loads from trabeculae to Ct bone, its properties remain fundamentally metabolic, with its greater surface area exposed to bone marrow than Ct bone. Thus, Ct bone should exhibit higher bone material properties than Tb bone, at equivalent tissue age. We found that the main difference in nanomechanical properties existing between Ct and Tb BSUs was the Indentation modulus, with higher values in Ct than in

**Table 2**
A–B. Pearson's correlations between nanoindentation, X-ray microradiography, Fourier transform infrared and Raman microspectroscopy variables, in each bone compartments, cortical (A), and trabecular (B).

A

| Cortical | Nanoindentation | | | Digitized microradiography | Infrared microspectroscopy | | | | | Raman microspectroscopy | | | | |
|---|---|---|---|---|---|---|---|---|---|---|---|---|---|---|
| | Indentation modulus | Hardness | Dissipated energy | Degree of mineralization | IR-Mineral/matrix | IR-Mineral maturity | IR-Crystallinity | IR-Carbonation | IR-Collagen maturity | Ram-Mineral/matrix | Ram-Crystallinity | Ram-Type B carbonates | Ram-Proline/hydroxyproline | Ram-PG/amides III |
| Indentation modulus | 1 | | | | | | | | | | | | | |
| Hardness | 0.798** | 1 | | | | | | | | | | | | |
| Dissipated energy | 0.748** | 0.752** | 1 | | | | | | | | | | | |
| Degree of mineralization | 0.573** | 0.729** | 0.677** | 1 | | | | | | | | | | |
| IR-Mineral/matrix | 0.565** | 0.775** | 0.702** | 0.856** | 1 | | | | | | | | | |
| IR-Mineral maturity | 0.632** | 0.711** | 0.739** | 0.742** | 0.811** | 1 | | | | | | | | |
| IR-Crystallinity | 0.585** | 0.590** | 0.679** | 0.724** | 0.779** | 0.754** | 1 | | | | | | | |
| IR-Carbonation | −0.542** | −0.524** | −0.606** | −0.658** | −0.710** | −0.798** | −0.711** | 1 | | | | | | |
| IR-Collagen maturity | 0.560** | 0.708** | 0.715** | 0.707** | 0.870** | 0.799** | 0.691** | −0.682** | 1 | | | | | |
| Raman-Mineral/matrix | 0.579** | 0.694** | 0.674** | 0.819** | 0.847** | 0.741** | 0.733** | −0.695** | 0.768** | 1 | | | | |
| Raman-Crystallinity | 0.598** | 0.708** | 0.659** | 0.840** | 0.817** | 0.728** | 0.644** | −0.657** | 0.733** | 0.877** | 1 | | | |
| Raman-Type B carbonates | 0.113 | 0.125 | 0.187 | 0.039 | 0.108 | 0.167 | 0.131 | −0.129 | 0.130 | 0.126 | −0.157 | 1 | | |
| Raman-Proline/hydroxyproline | −0.307** | −0.073 | −0.125 | 0.067 | 0.086 | 0.025 | −0.110 | 0.004 | 0.150 | −0.106 | −0.008 | −0.162 | 1 | |
| Raman-PG/amides III | −0.339** | −0.254** | −0.385** | −0.264** | −0.345** | −0.417** | −0.419** | 0.425** | −0.347** | −0.334** | −0.213** | −0.473** | 0.390** | 1 |

B

| Trabecular | Nanoindentation | | | Digitized microradiography | Infrared microspectroscopy | | | | | Raman microspectroscopy | | | | |
|---|---|---|---|---|---|---|---|---|---|---|---|---|---|---|
| | Indentation modulus | Hardness | Dissipated energy | Degree of mineralization | IR-Mineral/matrix | IR-Mineral maturity | IR-Crystallinity | IR-Carbonation | IR-Collagen maturity | Ram-Mineral/matrix | Ram-Crystallinity | Ram-Type B carbonates | Ram-Proline/hydroxyproline | Ram-PG/amides III |
| Indentation modulus | 1 | | | | | | | | | | | | | |
| Hardness | 0.815** | 1 | | | | | | | | | | | | |
| Dissipated energy | 0.722** | 0.783** | 1 | | | | | | | | | | | |
| Degree of mineralization | 0.575** | 0.678** | 0.684** | 1 | | | | | | | | | | |
| IR-Mineral/matrix | 0.674** | 0.790** | 0.802** | 0.816** | 1 | | | | | | | | | |
| IR-Mineral maturity | 0.639** | 0.657** | 0.733** | 0.642** | 0.792** | 1 | | | | | | | | |
| IR-Crystallinity | 0.506** | 0.612** | 0.639** | 0.644** | 0.808** | 0.758** | 1 | | | | | | | |
| IR-Carbonation | −0.583** | −0.521** | −0.633** | −0.652** | −0.675** | −0.768** | −0.657** | 1 | | | | | | |
| | 0.686** | 0.775** | 0.820** | 0.744** | 0.905** | 0.769** | 0.690** | −0.666** | 1 | | | | | |

(*continued on next page*)

**Table 2** (*continued*)

| B | | | | | | | | | | | | | |
|---|---|---|---|---|---|---|---|---|---|---|---|---|---|
| Trabecular | Nanoindentation | | | Digitized microradiography | Infrared microspectroscopy | | | | | Raman microspectroscopy | | | | |
| | Indentation modulus | Hardness | Dissipated energy | Degree of mineralization | IR-Mineral/matrix | IR-Mineral maturity | IR-Crystallinity | IR-Carbonation | IR-Collagen maturity | Ram-Mineral/matrix | Ram-Crystallinity | Ram-Type B carbonates | Ram-Proline/hydroxyproline | Ram-PG/amides III |
| IR-Collagen maturity | | | | | | | | | | | | | | |
| Raman-Mineral/matrix | 0.640** | 0.728** | 0.750** | 0.791** | 0.868** | 0.690** | 0.734** | −0.658** | 0.810** | 1 | | | | |
| Raman-Crystallinity | 0.554** | 0.605** | 0.636** | 0.759** | 0.801** | 0.575** | 0.678** | −0.583** | 0.752** | 0.884** | 1 | | | |
| Raman-Type B carbonates | 0.366** | 0.450** | 0.408** | 0.235** | 0.348** | 0.534** | 0.274** | −0.289** | 0.309** | 0.281** | 0.015 | 1 | | |
| Raman-Proline/hydroxyproline | 0.022 | 0.045 | −0.002 | 0.213 | 0.124 | 0.120 | −0.101 | −0.07 | 0.223* | 0.048 | 0.061 | 0.018 | 1 | |
| Raman-PG/amides III | −0.205** | −0.246** | −0.253** | −0.118 | −0.250** | −0.351** | −0.272** | 0.351** | −0.191** | −0.270** | −0.093 | −0.395** | 0.344** | 1 |

* $p < 0.05$.
** $p < 0.01$.

Tb BSUs, both in Ost and Int. Hardness was not different between Ost Ct and Ost Tb BSUs, or between Int Ct and Int Tb BSUs. Dissipated energy was higher in Int Ct BSUs than Int Tb BSUs. Regarding the mineral properties, unexpectedly, the DMB was found lower in Ct than Tb BSUs, both in Ost and Int bone, also confirmed by the measurement of the mineral/matrix by Raman and FTIRM spectroscopy (not significant in Ost). Higher mineral maturity (Ost and Int) and collagen maturity (Ost only), was found in Ct than in Tb BSUs. The higher mechanical properties between Ct and Tb bone, despite a lower mineralization, might be related to a different hierarchical arrangement of collagen fibrils between both compartments (oriented along the Haversian channel in Ct vs rod and plates in Tb).

Regarding the mineral content, a higher mineral content was expected in Ct bone than Tb, categorized by "tissue age". However, we found a slightly lower (or no different) mineral content, depending on the methods used: a lower mineral/matrix ratio was found in Ct than Tb both Ost and Int by Raman, a lower absolute degree of mineralization in both Ost and Int by microradiography, and a lower mineral/matrix ratio by FTIRM in Ct than in Tb (Int bone). While mineral/matrix by FTIRM and Raman is a relative ratio (amount of mineral by amount of organic matrix), and DMB measured by X ray microradiography an absolute ratio (volume of mineral on a given thickness), the 3 methods showed the same trend, i.e. a lower mineral content in Ct than Tb bone. We observed important variations of this variable in % between Ost and Int according to the technique used. These differences can be explained by 2 reasons: 1 - Regarding FTIRM and Raman spectroscopies, by a different vibration analysis between the 2 techniques (FTIRM: $PO_4$/amide I; Raman $PO_4/CH_2$), 2 - Regarding FTIRM/Raman versus X-ray microradiography, by a different principle of analysis: The P-O vibration is analysed by vibrational spectroscopy, versus the density of mineral (Ca, P and others mineral ions present in the apatite crystals) is measured by X-ray microradiography. The 3 techniques are complementary, by giving different information on the mineral content of bone, and showed a slightly lower mineral content in Ct versus Tb bone. That means that, for a same "range of BSUs tissue age", fewer apatite crystals were deposited in Ct than in Tb bone. However, this difference is weak compared to the differences found between Ost and Int. The reason why the mineralization of BSUs in Ct bone is lower than in Tb bone is unclear, as the mineral deposition kinetics is the same in both compartments. Indeed, the mineralization apposition rate (MAR) measured in Ct and Tb from bone biopsies taken from untreated PMOP women was not different in both compartments (MAR medians: 0.64 μm/day in Ct and 0.61 μm/day in Tb) (Chavassieux et al., 2019). One explanation could be the better accessibility of Ca and P ions from the bone marrow in the Tb bone than in Ct bone, due to the larger surface exposed to the bone marrow. An alternative explanation could be that the regulation of the crystals deposition is different between Ct and Tb; at the Ct envelope scale, the mineralization is higher than the Tb envelope (confirmed in this study with the DMB measured on the same bone biopsies and in previous study in a same population of PMOP women) (Farlay et al., 2019), due to a higher proportion of Int bone than Ost in Ct bone than in Tb bone. Thus, a mechanism of regulation of mineralization at the BSU scale could exist to avoid that the Ct bone become too mineralized.

Another variable important to assess is the crystallinity (crystal size and perfection) (Farlay et al., 2010). Bone crystals are nanosized platelet-shaped (length ≈ 20–60 nm, width ≈ 10–20 nm, thickness ≈ 2–5 nm) (Bala et al., 2013). While mineral maturity and crystallinity are often correlated, they reflect different characteristics. The mineral maturity reflects a stage of maturation. The crystallinity reflects the size/organization of apatite lattice. The crystallinity can be influenced by ionic substitutions whereas the mineral maturity cannot. The difference between Ost and Int BSUs was about 7 % by FTIRM and 5 % by Raman. We did not find differences between Ct and Tb bone by FTIRM, and a small difference (<1 %) by Raman. The difference in crystal size/perfection of bone apatite crystals between Ct and Tb bone is thus likely relatively small between both compartments.

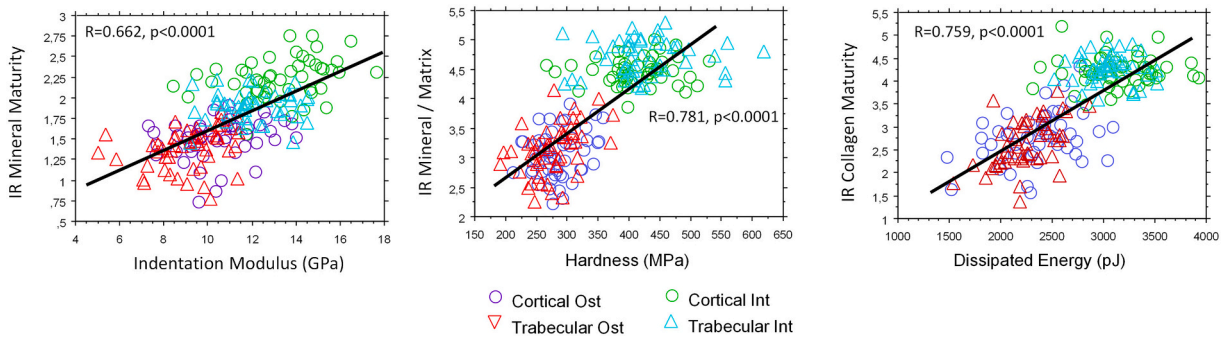


**Fig. 5.** Correlations between the nanomechanical and intrinsic variables in the 4 compartments. Each point is the mean of 10 and 5 BSUs for FTIRM and nanoindentation, respectively (n = 50 bone biopsies).

**Table 3**
Multiple regression analysis performed in each bone compartment: cortical (interstitial and osteonal), and trabecular (interstitial and osteonal).

| | | Cortical | | | | Trabecular | | | |
|---|---|---|---|---|---|---|---|---|---|
| | | Stepwise regression rank | Part correlation (β) | p-Value | Adjusted $R^2$ | Stepwise regression rank | Part correlation (β) | p-Value | Adjusted $R^2$ |
| Indentation modulus | Mineral/matrix | Out | – | – | 0.415 | Out | – | – | 0.491 |
| | Mineral maturity | 1 | 0.441 | <0.0001 | | 2 | 0.275 | 0.016 | |
| | Crystallinity | 2 | 0.253 | 0.033 | | Out | | | |
| | Collagen maturity | Out | – | – | | 1 | 0.474 | <0.0001 | |
| Hardness | Mineral/matrix | 1 | 0.581 | <0.0001 | 0.613 | 1 | 0.487 | 0.001 | 0.637 |
| | Mineral maturity | 2 | 0.24 | 0.027 | | Out | – | – | |
| | Crystallinity | Out | – | – | | 2 | 0.334 | 0.021 | |
| | Collagen maturity | Out | – | – | | – | – | – | |
| Dissipated energy | Mineral/matrix | Out | – | – | 0.597 | – | – | – | 0.692 |
| | Mineral maturity | 1 | 0.34 | 0.005 | | 2 | 0.252 | 0.005 | |
| | Crystallinity | 3 | 0.224 | 0.027 | | – | – | – | |
| | Collagen maturity | 2 | 0.288 | 0.01 | | 1 | 0.626 | <0.0001 | |

Mineral maturity, which assessed the conversion of non apatitic phosphates from the hydrated layer into apatitic phosphates in the crystal core (Farlay et al., 2010) was found higher in Ct BSUs than in Tb BSUs. However, crystallinity and mineral/matrix ratio were not higher in Ct bone than in Tb bone, indicating that the highest values of mineral maturity are not followed by increase in other variables as usually found. The mineral maturity reflects the ratio between $PO_4$ in crystal core over $PO_4$ in the hydrated layer and the $PO_4$ in crystal core directly influences the crystallinity. If the $PO_4$ in crystal core is the same, that would suggest the $PO_4$ in the hydrated layer is lower. As the latter is influenced by the level of hydration of bone matrix, this might suggest that the hydrated layer in Ct is less abundant than in BSUs in Tb bone. Ct bone has a lower water content (free + bound water) (Oftadeh et al., 2015; Granke et al., 2015) than Tb bone, leading Ct bone to fewer exchange surfaces with water. This could influence the level of mineral maturity in Ct bone (Ct BSU more "mature" than Tb). This suggests that the apatite crystals would be more mature in Ct than in Tb bone, for a similar crystal size/perfection.

Total carbonation assessed by FTIRM was lower in Int than Ost bone (about 15 %), in agreement with data generally observed by FTIRM (decrease with Carbonate to mineral ratio decreases as the tissue ages) (Gamsjaeger et al., 2014) while by Raman (type-B carbonates), the difference was weak, between 1.1 % and 3 %. There is a controversy in the literature on the evolution of carbonates in bone mineral with maturation. In synthetic apatites, both $CO_3/PO_4$ ratios measured by Raman or FTIRM positively correlated with gold-standard analytical measurements of carbonate content (Taylor et al., 2021). However, and depending on the age of the donor or the tissue age, the evolution of $CO_3/PO_4$ ratio is different, with lower level in bone from child compared to adults, and for both a higher $CO_3/PO_4$ ratio in Ost than Int bone (Lefèvre et al., 2019). The role of carbonates in bone strength is not yet fully elucidated.

Regarding the collagen maturity, slightly higher values were found in Ct Ost versus Tb Ost, without difference in Int. Those values are very weak compared to the differences found between Ost and Int bone. This result is in agreement with a previous study showing a strong correlation between the mineral content and the age of bone tissue, while no correlation was found with enzymatic cross-links (Farlay et al., 2011). PG/amides III were found lower in Int than Ost bone, in agreement with their ability to regulate negatively the mineralization by affecting apatite nucleation and growth. The relative PG content represents a part of noncollagenous compartment in bone. PG/amides II were lower in Ct Int than in Tb Int (no difference in Ost), while the mineral content was lower, indicating a difference in the PG/amides III in the matrix composition between Ct Int and Tb Int.

We found that Ct bone was more elastic than Tb bone, both in Ost (+17 %) and Int bone (+10.3 %). This difference was weak compared to the difference found between Ost and Int bone (+35.6 % in Cort, +27.4 % in Trab). Some studies showed a higher Young modulus in Ct than in Tb bone (Rho et al., 1999c; Rho et al., 1997), others showed no difference (Turner et al., 1999), or lower elastic modulus in Ct than in Tb bone (Hengsberger et al., 2001), due to the difficulty to compare similar structures. The indentation modulus values were similar to those found in femur in wet conditions [in neck Tb (8–18 GPa), in neck Ct (12–20

GPa) (Hengsberger et al., 2002), or in Tb bone (11.4 GPa) (Zysset et al., 1999)] or transiliac bone with osteomalacia in the mineral part (Hadjab et al., 2021) (12.2 GPa). Depending on the studies, conditions of sample preparation or analysis conditions (wet vs dry) (Zysset, 2009; Hengsberger et al., 2002; Bushby et al., n.d.; Wolfram et al., 2010), orientation of bone (transverse or longitudinal) (Rho et al., 1997; Rho et al., 1999c; Rho et al., 1999b; Zysset et al., 1999; Fan et al., 2002; Goodwin and Sharkey, 2002), the elastic modulus of human Tb bone may vary between 6.9 and 32.3 GPa (Zysset, 2009; Zysset et al., 1999; Thurner, 2009; Donnelly et al., 2006), and between 17 and 27 GPa (femur midshaft) in Ct bone (Thurner, 2009). Moreover, elastic modulus has been shown to be correlated to the mineral content (in calcified cartilage) (Gupta et al., 2005), while not always (Spiesz et al., 2013). Two hypotheses could explain the higher values in Ct than in Tb bone: 1 - Ct bone contains less matrix-bound-water than Tb bone (as all experiments were performed in hydrated conditions). As elastic modulus is higher when bone hydration is low (Granke et al., 2015; Faingold et al., 2014), this could be due to the stiffening of the collagen phase or/and a lower distance between collagen and mineral upon dehydration (Rai and Sinha, 2011) 2 - The concentric structure of lamellae in Ct (tested in transverse direction only) may influence the elastic properties, as the Tb bone was tested randomly in different orientations. This emphasize to take into account the "tissue age of bone" and to compare similar microstructure in the assessment of nanomechanical properties of Ct and Tb bone.

Difference in hardness was not found between Ct and Tb bone when categorized by "tissue age". This is in agreement with our previous study performed by microindentation (Boivin et al., 2008b). For comparison, the difference of hardness found between Ost and Int bone was 46.5 % in Ct, +55.1 % in Tb. As the mineralization was slightly lower in Ct than in Tb bone, we could expect a lower microhardness. However, hardness mainly depends on the degree of mineralization but also on the orientation and arrangement of collagen fibres (Zysset, 2009; Amprino, 1958; Ziv et al., 1996), and this could explain the absence of difference of hardness between Ct and Tb bone. Some studies reported difference in hardness with higher values in Ct than Tb, but the BSUs were not chosen with a similar "age", thus the increase in hardness reflected the higher proportion of Int bone than Ost bone in cortical (Hodgskinson et al., 1989). However, we acknowledge that relating tissue-level differences to whole bone mechanics is a challenge.

Energy dissipation in bone is a mechanism allowing to maximize the fracture resistance through different mechanisms of permanent deformations (microcracking, damage in collagen and crosslinking, sliding of collagen molecules, sliding of collagen between apatite crystal and collagen molecules). The energy dissipation, a viscoelastic phenomenon, mainly depends on the viscous phases (collagen and water). However, introduction of mineral leads to an increase in energy dissipation, as shown using a computational model (Buehler, 2007a; Depalle et al., 2016). Up to five different deformation mechanisms to dissipate energy in bone have been identified (molecular uncoiling, molecular stretching, mineral/collagen sliding, molecular slippage, and crystal dissociation) (Depalle et al., 2016). Thus, the energy dissipation is a complex phenomenon, implying in a strongly intricate way, the interaction between organic, mineral, and water components. Dissipated energy was higher in Ct than Tb bone (+3.6 %; $p = 0.0255$), in Int bone only (trend in Ost). This difference being relatively weak since the difference Int versus Ost is much higher (36–37 % higher in Int than Ost). Depending on the bone compartments analysed, we observed the contribution in this process of either bone mineral or organic phase. Other components, not measured here, are implied in the dissipation of energy, as shown by Nyman et al. with non-enzymatic cross-links (Pentodisine, inversely correlated with post-yield energy dissipation) (Nyman et al., 2007), or by Nikel et al. with the role of non-collagenous proteins (KO mice for Osteocalcin and osteopontin) and the ionic interactions of their charged side chains on hydrogen bonding to dissipate energy in bone (Nikel et al., 2018).

In order to explain the contribution of mineral and organic properties in the nanomechanical variables, a multiple regression analysis was performed with FTIRM data. In Ct bone, the indentation modulus was explained by mineral maturity and crystallinity, two variables related to apatite crystal maturation. In contrast, in Tb bone, indentation modulus was explained first by collagen maturity then by mineral maturity. We did also not find contribution of mineral content (mineral/matrix ratio) in indentation modulus in either Ct or Tb. In our study, the maturation of individual crystals prevails over the mineral content in the indentation modulus. This could suggest that the maturation of each individual platelet is a fundamental element in bone strength, more important than the mineral content. The maturation of each individual crystal leads to the formation of very rigid individual platelets, with a high density of covalent ions inside the collagen fibrils (Buehler, 2007a). By a combination of molecular dynamics simulation and theoretical analysis, Buehler (2007b) showed that the increase of the strength was related to the molecular role of apatite platelets in mineralized collagen fibrils, by providing a larger energy barrier against intermolecular slip. In a study on tibia, Choi et al. (1990) showed the difference in the modulus between Ct and Tb bone (lower in Tb than Ct) was not explained by the mineral content, and suggested that microstructural differences as the lamellar/collagen organization and orientation could be potent determinants of young modulus. Indentation modulus, which basically describes how well the bone resists to deformation under stress, is inherently related to atomic bonding, and is related to the number of bonds per atom along with their stiffness. In Ct, indentation modulus would be mainly influenced by mineral features (bonding/interactions between mineral crystals and collagen) whereas in Tb, indentation modulus would rather be influenced by collagen feature (collagen fibres packing). The different lamellae disposition between Ct and Tb (concentric lamellae versus angular segments of parallel sheets) could explain those different properties. As explained before, the higher mineral maturity in Ct could be due to lower water content compared to Tb, and associated to the more compact structure of concentric lamellae, this could lead to stiffening of the atomic bonds by reducing the distance between mineral crystals and or collagen/mineral crystals. The contribution of mineral in the indentation modulus would thus be more pronounced in Ct than in Tb bone, in which the packets are unrolled on the bone marrow. In a previous study by instrumented microindentation in Ct bone, indentation modulus was explained in part by the DMB in dry conditions (Bala et al., 2011). Thus, the different results with the present study can be due to the difference in analysis conditions (wet in the present study versus dry (Bala et al., 2011)). Indeed, as indentation modulus is strongly influenced by the state of hydration, intrinsic mineral variables other than the degree of mineralization may appear correlated with these nanomechanical properties. The hardness, on the other hand, was explained by the mineral/matrix ratio both in Ct and Tb, followed by mineral maturity or crystallinity in Ct and Tb, respectively. The mineral content is the main determinant of the bone hardness, which is in agreement with data generally reported in the literature (Boivin et al., 2008a; Zysset et al., 1999). The dissipated energy was first explained, depending on the compartment, by either mineral maturity (Ct) or collagen maturity (Tb), followed by collagen maturity and crystallinity in Ct and by mineral maturity in Tb. The different composition and the different microstructure structure between Ct and Tb BSUs could explain those differences. All the correlations values were positive, indicating that the maturation of both organic and mineral matrix improve the dissipation of energy. As recently shown, the collagen is the component "primarily responsible for dissipating energy, upon transient loads" (Milazzo et al., 2020) but other studies have also shown the role of mineral in the strengthening of the collagen and the role of hydration in the toughness of bone (Fielder and Nair, 2019; Buehler, 2007a). By a combination of molecular dynamics simulation and theoretical analysis, Buehler (2007a) showed that the introduction of mineralization in collagen fibrils leaded to a factor of 5 increase on energy dissipation, revealing "how a highly dissipative but strong material, can be formed from soft collagen fibrils, and hard and brittle apatite by a hierarchical

optimized arrangement between collagen and apatite crystals, at nanostructured length scale". To achieve it, ionic interactions across collagen-mineral allow obtaining the critical adhesion energy. This makes it more difficult to initiate molecular slip, but is small enough so that covalent bonds inside collagen molecules are not broken. The maturation and growth of apatite crystals allow increasing the interface energy with collagen fibrils, by increasing the contact surface between both components, allowing to improve the mechanisms of energy dissipation.

This study has some strengths and limitations. The major strength is that 50 to 60 bone biopsies were analysed, with 2000 to 2400 BSUs assessed, depending on the techniques used. The main limitation is that this study has been conducted on osteoporotic bone from post-menopausal women, and this cannot be extrapolated to healthy bone. Moreover, the different analyses were not performed on the same BSUs, but categorized by Ost of Int BSUs, that can weaken the differences and correlations. Another limitation is that the comparison of micro-mechanical properties between Ct and Tb is weaken by the different collagen orientation, and this can hampers the conclusion. The levels of AGEs and enzymatic crosslinks were not assessed even if they possibly affect nanomechanical properties of bone. As iliac crest is not a weight bearing bone, it may be not representative of other bone and some different results could be observed.

In conclusion, differences exist between Ct and Tb bone based on the evaluation of the mechanical and matrix properties at BSUs level, in human iliac bone, the most important being related to elastic modulus and mineral maturity. However, these differences are weak compared to those observed between Ost and Int bone. As the level of bone remodeling activity influences the proportion of the ratio Ost/Int BSUs (higher remodeling activity stimulates the production of Ost BSUs), Ct and Tb bone mechanical properties will thus mainly depend on this proportion. Higher level of bone remodeling activity will lead to a lower Ct and Tb bone stiffness, hardness and dissipated energy. Moreover, the respective volume of Ct and Tb bone will also influence the whole bone strength, since Ct bone has higher indentation modulus and mineral maturity than Tb bone. Thus, if the Ct volume is too low compared to Tb bone, this will have a negative impact on whole bone strength and bone will be more prone to fracture. Those findings could help to build microfinite element modeling for fracture risk prediction.

## CRediT authorship contribution statement

Conceptualization and design: DF, GF, GB, PA. Acquisition of the data: DF, GF, CP, SR, IB. Analysis and interpretation of the data: DF, GF, CP, GP, IB, PA, GB. Statistical analysis: DF, GF. Writing-original draft: DF. Writing-review and editing: DF, GF, BC, RC, GP, GB. Revising and final approval: DF, GF, CP, SR, BC, RC, GP, IB, PA, GB.

## Declaration of competing interest

Delphine Farlay, Guillaume Falgayrac, Camille Ponçon, Sébastien Rizzo, Bernard Cortet, Roland Chapurlat, Guillaume Penel, Isabelle Badoud, Patrick Ammann and Georges Boivin declare that they have no conflicts of interest.

## Data availability

Data will be made available on request.

## Acknowledgements

The authors acknowledge the Institut de Recherches Internationales Servier (Suresnes, France), and especially Agnès Lalande, for providing the samples for this study and for their financial support.

## References

Ammann, P., Badoud, I., Barraud, S., Dayer, R., Rizzoli, R., 2007. Strontium ranelate treatment improves trabecular and cortical intrinsic bone tissue quality, a determinant of bone strength. J. Bone Miner. Res. 22 (9), 1419–1425. Sep.

Amprino, R., 1958. Investigations on some physical properties of bone tissue. Acta Anat. (Basel) 34 (3), 161–186.

Ascenzi, A., Bonucci, E., 1968. The compressive properties of single osteons. Anat. Rec. 161 (3), 377–391. Jul.

Bala, Y., Depalle, B., Douillard, T., Meille, S., Clément, P., Follet, H., Chevalier, J., Boivin, G., 2011. Respective roles of organic and mineral components of human cortical bone matrix in micromechanical behavior: an instrumented indentation study. J. Mech. Behav. Biomed. Mater. 4 (7), 1473–1482. Oct.

Bala, Y., Farlay, D., Boivin, G., 2013. Bone mineralization: from tissue to crystal in normal and pathological contexts. Osteoporos. Int. 24 (8), 2153–2166. Aug.

Bayraktar, H.H., Morgan, E.F., Niebur, G.L., Morris, G.E., Wong, E.K., Keaveny, T.M., 2004. Comparison of the elastic and yield properties of human femoral trabecular and cortical bone tissue. J. Biomech. 37 (1), 27–35. Jan.

Boivin, G., Meunier, P.J., 2003. The mineralization of bone tissue: a forgotten dimension in osteoporosis research. Osteoporos. Int. 14 (Suppl. 3), S19–S24.

Boivin, G., Bala, Y., Doublier, A., Farlay, D., Ste-Marie, L.G., Meunier, P.J., Delmas, P.D., 2008. The role of mineralization and organic matrix in the microhardness of bone tissue from controls and osteoporotic patients. Bone 43 (3), 532–538. Sep 1.

Boivin, G., Bala, Y., Doublier, A., Farlay, D., Ste-Marie, L.G., Meunier, P.J., Delmas, P.D., 2008. The role of mineralization and organic matrix in the microhardness of bone tissue from controls and osteoporotic patients. Bone 43 (3), 532–538. Sep.

Buehler, M.J., 2007a. Molecular nanomechanics of nascent bone: fibrillar toughening by mineralization. IOP Publishing Nanotechnology 18 (29), 295102. Jun.

Buehler, M.J., 2007b. Molecular nanomechanics of nascent bone: fibrillar toughening by mineralization. Nanotechnology 18. https://doi.org/10.1088/0957-4484/18/29/295102.

Burr, D.B., 2011. Why bones bend but don't break. J. Musculoskelet. Neuronal Interact. 11 (4), 270–285. Dec.

Bushby A, Ferguson V, Boyde A. Nanoindentation of bone: comparison of specimens tested in liquid and embedded in polymethylmethacrylate. J. Mater. Res. 19(1): 249–59.

Cazalbou, S., Combes, C., Eichert, D., Rey, C., Glimcher, M.J., 2004. Poorly crystalline apatites: evolution and maturation in vitro and in vivo. J. Bone Miner. Metab. 22 (4), 310–317.

Chavassieux, P., Meunier, P.J., Roux, J.P., Portero-Muzy, N., Pierre, M., Chapurlat, R., 2014. Bone histomorphometry of transiliac paired bone biopsies after 6 or 12 months of treatment with oral strontium ranelate in 387 osteoporotic women: randomized comparison to alendronate. J. Bone Miner. Res. 29 (3), 618–628. Mar.

Chavassieux, P., Chapurlat, R., Portero-Muzy, N., Roux, J.-P., Garcia, P., Brown, J.P., Libanati, C., Boyce, R.W., Wang, A., Grauer, A., 2019. Bone-forming and antiresorptive effects of romosozumab in postmenopausal women with osteoporosis: bone histomorphometry and microcomputed tomography analysis after 2 and 12 months of treatment. J. Bone Miner. Res. 34 (9), 1597–1608. Sep.

Choi, K., Kuhn, J.L., Ciarelli, M.J., Goldstein, S.A., 1990. The elastic moduli of human subchondral, trabecular, and cortical bone tissue and the size-dependency of cortical bone modulus. J. Biomech. 23 (11), 1103–1113.

Currey, J.D., 2002. Bones: Structure and Mechanics. Princeton University Press, Princeton.

Davies, E., Müller, K.H., Wong, W.C., Pickard, C.J., Reid, D.G., Skepper, J.N., Duer, M.J., 2014. Citrate bridges between mineral platelets in bone. Proc. Natl. Acad. Sci. U. S. A. 111 (14), E1354–E1363. Apr 8.

Depalle, B., Qin, Z., Shefelbine, S.J., Buehler, M.J., 2016. Large deformation mechanisms, plasticity, and failure of an individual collagen fibril with different mineral content. J. Bone Miner. Res. 31 (2), 380–390. Feb.

Donnelly, E., Baker, S.P., Boskey, A.L., van der Meulen, M.C.H., 2006. Effects of surface roughness and maximum load on the mechanical properties of cancellous bone measured by nanoindentation. J. Biomed. Mater. Res. A 77 (2), 426–435. May.

Faingold, A., Cohen, S.R., Shahar, R., Weiner, S., Rapoport, L., Wagner, H.D., 2014. The effect of hydration on mechanical anisotropy, topography and fibril organization of the osteonal lamellae. J. Biomech. 47 (2), 367–372. Jan 22.

Falgayrac, G., Cortet, B., Devos, O., Barbillat, J., Pansini, V., Cotten, A., Pasquier, G., Migaud, H., Penel, G., 2012. Comparison of two-dimensional fast raman imaging versus point-by-point acquisition mode for human bone characterization. Anal. Chem. 84 (21), 9116–9123. Nov 6.

Falgayrac, G., Farlay, D., Ponçon, C., Béhal, H., Gardegaront, M., Ammann, P., Boivin, G., Cortet, B., 2021. Bone matrix quality in paired iliac bone biopsies from postmenopausal women treated for 12 months with strontium ranelate or alendronate. Bone 11 (153), 116107. Jul.

Fan, Z., Swadener, J.G., Rho, J.Y., Roy, M.E., Pharr, G.M., 2002. Anisotropic properties of human tibial cortical bone as measured by nanoindentation. J. Orthop. Res. 20 (4), 806–810. Jul.

Fan, Z., Smith, P.A., Eckstein, E.C., Harris, G.F., 2006. Mechanical properties of OI type III bone tissue measured by nanoindentation. J. Biomed. Mater. Res. A 79 (1), 71–77. Oct.

Fan, Z., Smith, P.A., Harris, G.F., Rauch, F., Bajorunaite, R., 2007. Comparison of nanoindentation measurements between osteogenesis imperfecta type III and type IV and between different anatomic locations (femur/tibia versus iliac crest). Connect. Tissue Res. 48 (2), 70–75.

Fantner, G.E., Hassenkam, T., Kindt, J.H., Weaver, J.C., Birkedal, H., Pechenik, L., Cutroni, J.A., Cidade, G.A.G., Stucky, G.D., Morse, D.E., Hansma, P.K., 2005.

Sacrificial bonds and hidden length dissipate energy as mineralized fibrils separate during bone fracture. Nat. Mater. 4 (8), 612–616. Aug.
Farlay, D., Panczer, G., Rey, C., Delmas, P.D., Boivin, G., 2010. Mineral maturity and crystallinity index are distinct characteristics of bone mineral. J. Bone Miner. Metab. 28 (4), 433–445. Jul.
Farlay, D., Duclos, M.-E., Gineyts, E., Bertholon, C., Viguet-Carrin, S., Nallala, J., Sockalingum, G.D., Bertrand, D., Roger, T., Hartmann, D.J., Chapurlat, R., Boivin, G., 2011. The ratio 1660/1690 cm(-1) measured by infrared microspectroscopy is not specific of enzymatic collagen cross-links in bone tissue. PLoS One 6 (12), e28736.
Farlay, D., Bala, Y., Rizzo, S., Bare, S., Lappe, J.M., Recker, R., Boivin, G., 2019. Bone remodeling and bone matrix quality before and after menopause in healthy women. Bone 128, 115030. Nov.
Fielder, M., Nair, A.K., 2019. Effects of hydration and mineralization on the deformation mechanisms of collagen fibrils in bone at the nanoscale. Biomech. Model. Mechanobiol. 18 (1), 57–68. Feb.
Fisher, L.W., Torchia, D.A., Fohr, B., Young, M.F., Fedarko, N.S., 2001. Flexible structures of SIBLING proteins, bone sialoprotein, and osteopontin. Biochem. Biophys. Res. Commun. 280 (2), 460–465. Jan 19.
Gamsjaeger, S., Mendelsohn, R., Boskey, A.L., Gourion-Arsiquaud, S., Klaushofer, K., Paschalis, E.P., 2014. Vibrational spectroscopic imaging for the evaluation of matrix and mineral chemistry. Curr. Osteoporos. Rep. 12 (4), 454–464. Dec.
Goodwin, K.J., Sharkey, N.A., 2002. Material properties of interstitial lamellae reflect local strain environments. J. Orthop. Res. 20 (3), 600–606. May.
Granke, M., Does, M.D., Nyman, J.S., 2015. The role of water compartments in the material properties of cortical bone. Calcif. Tissue Int. 97 (3), 292–307. Sep.
Gupta, H.S., Schratter, S., Tesch, W., Roschger, P., Berzlanovich, A., Schoeberl, T., Klaushofer, K., Fratzl, P., 2005. Two different correlations between nanoindentation modulus and mineral content in the bone-cartilage interface. J. Struct. Biol. 149 (2), 138–148. Feb.
Hadjab, I., Farlay, D., Crozier, P., Douillard, T., Boivin, G., Chevalier, J., Meille, S., Follet, H., 2021. Intrinsic properties of osteomalacia bone evaluated by nanoindentation and FTIRM analysis. J. Biomech. 5 (117), 110247. Mar.
Hengsberger, S., Kulik, A., Zysset, P., 2001. A combined atomic force microscopy and nanoindentation technique to investigate the elastic properties of bone structural units. Eur. Cell Mater. 10 (1), 12–17. Jan.
Hengsberger, S., Kulik, A., Zysset, P., 2002. Nanoindentation discriminates the elastic properties of individual human bone lamellae under dry and physiological conditions. Bone 30 (1), 178–184. Jan.
Hengsberger, S., Ammann, P., Legros, B., Rizzoli, R., Zysset, P., 2005. Intrinsic bone tissue properties in adult rat vertebrae: modulation by dietary protein. Bone 36 (1), 134–141. Jan.
Hodgskinson, R., Currey, J.D., Evans, G.P., 1989. Hardness, an indicator of the mechanical competence of cancellous bone. J. Orthop. Res. 7 (5), 754–758.
Hoffler, C.E., Moore, K.E., Kozloff, K., Zysset, P.K., Goldstein, S.A., 2000. Age, gender, and bone lamellae elastic moduli. J. Orthop. Res. 18 (3), 432–437. May.
Hu, Y.-Y., Rawal, A., Schmidt-Rohr, K., 2010. Strongly bound citrate stabilizes the apatite nanocrystals in bone. Proc. Natl. Acad. Sci. U. S. A. 107 (52), 22425–22429. Dec 28.
Hunter, G.K., Goldberg, H.A., 1993. Nucleation of hydroxyapatite by bone sialoprotein. Proc. Natl. Acad. Sci. U. S. A. 90 (18), 8562–8565. Sep 15.
Lefèvre, E., Farlay, D., Bala, Y., Subtil, F., Wolfram, U., Rizzo, S., Baron, C., Zysset, P., Pithioux, M., Follet, H., 2019. Compositional and mechanical properties of growing cortical bone tissue: a study of the human fibula. Sci. Rep. 26;9 (1), 17629.
Lespessailles, E., Hambli, R., Ferrari, S., 2016. Osteoporosis drug effects on cortical and trabecular bone microstructure: a review of HR-pQCT analyses. Bonekey Rep. 31 (5), 836. Aug.
Milazzo, M., Jung, G.S., Danti, S., Buehler, M.J., 2020. Mechanics of mineralized collagen fibrils upon transient loads. ACS Nano 14 (7), 8307–8316. Jul 28.
Mirzaali, M.J., Schwiedrzik, J.J., Thaiwichai, S., Best, J.P., Michler, J., Zysset, P.K., Wolfram, U., 2016. Mechanical properties of cortical bone and their relationships with age, gender, composition and microindentation properties in the elderly. Bone 93, 196–211. Dec.
Montagner, F., Kaftandjian, V., Farlay, D., Brau, D., Boivin, G., Follet, H., 2015. Validation of a novel microradiography device for characterization of bone mineralization. J. Xray Sci. Technol. 23 (2), 201–211.
Nikel, O., Poundarik, A.A., Bailey, S., Vashishth, D., 2018. Structural role of osteocalcin and osteopontin in energy dissipation in bone. J. Biomech. 26 (80), 45–52. Oct.
Nyman, J.S., Roy, A., Shen, X., Acuna, R.L., Tyler, J.H., Wang, X., 2006. The influence of water removal on the strength and toughness of cortical bone. J. Biomech. 39 (5), 931–938.
Nyman, J.S., Roy, A., Acuna, R.L., Gayle, H.J., Reyes, M.J., Tyler, J.H., Dean, D.D., Wang, X., 2006. Age-related effect on the concentration of collagen crosslinks in human osteonal and interstitial bone tissue. Bone 39 (6), 1210–1217. Dec.
Nyman, J.S., Roy, A., Tyler, J.H., Acuna, R.L., Gayle, H.J., Wang, X., 2007. Age-related factors affecting the postyield energy dissipation of human cortical bone. J. Orthop. Res. 25 (5), 646–655.
Oftadeh, R., Perez-Viloria, M., Villa-Camacho, J.C., Vaziri, A., Nazarian, A., 2015. Biomechanics and mechanobiology of trabecular bone: a review. J. Biomech. Eng. 137 (1). Jan.
Qiu, S.R., Wierzbicki, A., Orme, C.A., Cody, A.M., Hoyer, J.R., Nancollas, G.H., Zepeda, S., De Yoreo, J.J., 2004. Molecular modulation of calcium oxalate crystallization by osteopontin and citrate. Proc. Natl. Acad. Sci. U. S. A. 101 (7), 1811–1815. Feb 17.
Rai, R.K., Sinha, N., 2011. Dehydration-induced structural changes in the collagen-hydroxyapatite Interface in bone by high-resolution solid-state NMR spectroscopy. J. Phys. Chem. C 115 (29), 14219–14227. Jul 28.
Rho, J.Y., Tsui, T.Y., Pharr, G.M., 1997. Elastic properties of human cortical and trabecular lamellar bone measured by nanoindentation. Biomaterials 18 (20), 1325–1330. Oct.
Rho, J.Y., Roy, M.E., Tsui, T.Y., Pharr, G.M., 1999. Elastic properties of microstructural components of human bone tissue as measured by nanoindentation. J. Biomed. Mater. Res. 45 (1), 48–54. Apr.
Rho, J.Y., Zioupos, P., Currey, J.D., Pharr, G.M., 1999. Variations in the individual thick lamellar properties within osteons by nanoindentation. Bone 25 (3), 295–300. Sep.
Rho, J.Y., Roy, M.E., Tsui, T.Y., Pharr, G.M., 1999. Elastic properties of microstructural components of human bone tissue as measured by nanoindentation. J. Biomed. Mater. Res. 45 (1), 48–54. Apr.
Roschger, P., Paschalis, E.P., Fratzl, P., Klaushofer, K., 2008. Bone mineralization density distribution in health and disease. Bone 42 (3), 456–466. Mar.
Roy, M.E., Rho, J.Y., Tsui, T.Y., Evans, N.D., Pharr, G.M., 1999. Mechanical and morphological variation of the human lumbar vertebral cortical and trabecular bone. J. Biomed. Mater. Res. 44 (2), 191–197. Feb.
Singleton, R.C., Pharr, G.M., Nyman, J.S., 2021. Increased tissue-level storage modulus and hardness with age in male cortical bone and its association with decreased fracture toughness. Bone 148, 115949. Jul.
Spiesz, E.M., Reisinger, A.G., Kaminsky, W., Roschger, P., Pahr, D.H., Zysset, P.K., 2013. Computational and experimental methodology for site-matched investigations of the influence of mineral mass fraction and collagen orientation on the axial indentation modulus of lamellar bone. J. Mech. Behav. Biomed. Mater. 28, 195–205. Dec.
Sroga, G.E., Karim, L., Colón, W., Vashishth, D., 2011. Biochemical characterization of major bone-matrix proteins using nanoscale-size bone samples and proteomics methodology. Mol. Cell. Proteomics 10 (9), M110.006718. Sep.
Taylor, E.A., Mileti, C.J., Ganesan, S., Kim, J.H., Donnelly, E., 2021. Measures of bone mineral carbonate content and mineral Maturity/Crystallinity for FT-IR and raman spectroscopic imaging differentially relate to physical-chemical properties of carbonate-substituted hydroxyapatite. Calcif. Tissue Int. 109 (1), 77–91. Jul.
Thurner, P.J., 2009. Atomic force microscopy and indentation force measurement of bone. Wiley Interdiscip. Rev. Nanomed. Nanobiotechnol. 1 (6), 624–649. Dec.
Turner, C.H., Rho, J., Takano, Y., Tsui, T.Y., Pharr, G.M., 1999. The elastic properties of trabecular and cortical bone tissues are similar: results from two microscopic measurement techniques. J. Biomech. 32 (4), 437–441. Apr.
Viguet-Carrin, S., Garnero, P., Delmas, P.D., 2006. The role of collagen in bone strength. Osteoporos. Int. 17 (3), 319–336.
Wang, Y., Von Euw, S., Fernandes, F.M., Cassaignon, S., Selmane, M., Laurent, G., Pehau-Arnaudet, G., Coelho, C., Bonhomme-Coury, L., Giraud-Guille, M.-M., Babonneau, F., Azaïs, T., Nassif, N., 2013. Water-mediated structuring of bone apatite. Nat. Mater. 12 (12), 1144–1153. Dec.
Wolfram, U., Wilke, H.-J., Zysset, P.K., 2010. Rehydration of vertebral trabecular bone: influences on its anisotropy, its stiffness and the indentation work with a view to age, gender and vertebral level. Bone 46 (2), 348–354. Feb.
Ziv, V., Wagner, H.D., Weiner, S., 1996. Microstructure-microhardness relations in parallel-fibered and lamellar bone. Bone 18 (5), 417–428. May.
Zysset, P.K., 2009. Indentation of bone tissue: a short review. Osteoporos. Int. 20 (6), 1049–1055. Jun.
Zysset, P.K., Guo, X.E., Hoffler, C.E., Moore, K.E., Goldstein, S.A., 1999. Elastic modulus and hardness of cortical and trabecular bone lamellae measured by nanoindentation in the human femur. J. Biomech. 32 (10), 1005–1012. Oct.